

Extending the Visco-Plastic Lubrication Concept to Near Net Shape Products and Encapsulation

Sarah Hormozi^{1,2}, Geoff Dunbrack¹, Ian A. Frigaard^{1,2}

¹Department of Mechanical Engineering, University of British Columbia, Canada.

²Department of Mathematics, University of British Columbia, Canada

ABSTRACT

We present preliminary results of experimental and computational studies targeted at extending the visco-plastic lubrication concept to near-net shape products and to the transport of encapsulated fluid droplets. By carefully controlling the flow rates of different fluid streams it appears possible to engineer wavy walled tubes/channels, inserts and to produce droplets of varying shapes. In all cases the yield stress of the fluids “freezes in” the interface shape between simultaneously pumped streams of two fluids. Length-scales are governed by the geometry of the forming device rather than by capillary phenomena. We discuss a range of potential industrial applications.

INTRODUCTION

Multi-layer shear flows have broad range of application in industry such as co-extrusion processes and lubricated pipelining. Particularly in co-extrusion operations, but also in other multi-layer flows, the rate of production is limited by flow instabilities and especially by instabilities at the interface between adjacent layers. In the case of a duct flow, it is known that use of a yield stress fluid as the lubricating fluid, coupled with maintaining a plug region at the interface can lead to flows that are hydro-dynamically stable. The basic idea is that the interfacial stress remains a

finite amount below the yield stress in such flows, which means they can withstand finite perturbations to the flow. Various studies have established the feasibility of these flows from theoretical^{1,2,3}, experimental^{4,5}, and computational^{6,7} perspectives. The methodology has been termed visco-plastic lubrication (VPL).

In this paper we present preliminary results of experimental and computational studies targeted at extending the viscoplastic lubrication concept to near-net shape products and to the transport of encapsulated fluid droplets. By carefully controlling the flow rates of different fluid streams it appears possible to engineer wavy walled tubes/channels, inserts and to produce droplets of varying shapes. In all cases the yield stress of the fluids “freezes in” the interface shape between simultaneously pumped streams of two fluids. Length-scales are governed by the geometry of the forming device rather than by capillary phenomena. We discuss a range of potential industrial applications.

BASIC IDEA

In a shear flow along a duct the shear stress increases from centre to edge. This is true also for multi-layer shear flows, provided the density difference is modest. The basic idea of visco-plastic lubrication is to setup a multi-layer shear flow in which one fluid has a yield stress and to position

that fluid in such a way that the fluid is unyielded at the interface (see Fig. 1a). In this idealised configuration only shear stresses are present in the flow and these lie below the yield stress by a finite amount at the interface, ensuring stability.

If now we slowly oscillate the flow rates, we can expect to preserve the unyielded nature of the fluid at the interface, while capturing the flow oscillations in the form of a *frozen* interfacial profile, formed in the entrance region and held in place by the yield stress (see Fig. 1a). If the amplitude of the flow rate oscillation is increased further, to the point where the central flow becomes zero for a time period, we may expect some form of encapsulation to occur.

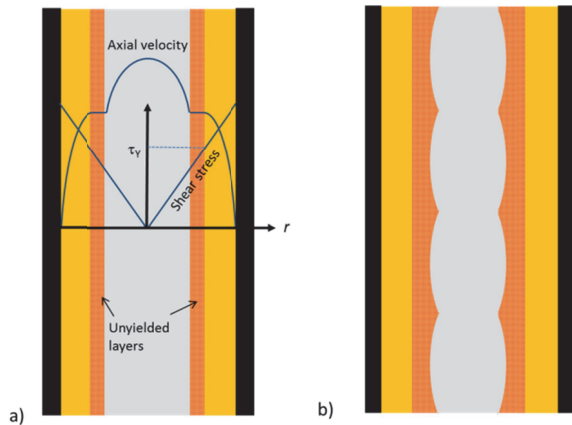


Figure 1. a) Schematic of the basic VPL idea; b) oscillations from the flow rate frozen in at the interface.

The flow transition between a frozen wavy-interface and complete encapsulation of the inner fluid in the form of droplets will be controlled by the wave-form of the oscillations imposed, by the underlying base flow and possibly by a form of pinch-off phenomenon. We have studied these effects both computationally and experimentally, and present our results below. Our physical understanding of these different processes is fairly preliminary and consequently our results are largely qualitative

COMPUTATIONS

Methodology:

For simplicity our computational work is carried out using a Bingham fluid model as the lubricating yield stress fluid and a Newtonian fluid as the core fluid. The fluids have identical density. A plane channel geometry is used, of dimensionless width 2, with the central inlet of width $2Y_i$, positioned symmetrically. The flow is governed by a Reynolds number Re , a Bingham number B and a viscosity ratio m . These are defined based on the total mean velocity of both fluids, the channel half-width and on the viscosity of the Newtonian fluid. The mathematical model is described in greater detail in our previous work.⁷

The computational method we use is largely as described in our previous work^{6,7}. The model equations consist of the Navier-Stokes equation coupled to a concentration equation. They are discretized using a mixed finite element/finite volume method. The computations are carried out on a structured rectangular mesh. The Navier-Stokes equations are solved using a semi-implicit Galerkin finite element method, where the divergence-free condition is enforced by an augmented Lagrangian technique. We regularise the effective viscosity functional to deal with yield stress fluid. The concentration equation is dealt with using a MUSCL scheme. On each timestep a splitting method is used to advance the concentration equation over a number of smaller sub-time steps, preserving stability. The numerical algorithm is implemented in C++ as an application of PELICANS⁸.

Near-net shape example flow results:

A vertically oriented channel is initially filled with Bingham fluid (fluid 2). For times $t > 0$ a Newtonian fluid (fluid 1) is injected upwards through a centrally positioned inner channel of width $2Y_i$, while at the same time the Bingham fluid is pumped through the outer part of the

channel, (see Fig. 1). Having established a steady multi-layer flow⁷, we then slightly perturb the flow rates of fluid 1 and fluid 2 while maintaining a constant total flow rate: $Q_1 + Q_2 = 1$, i.e. $Q_1 \rightarrow Q_1 + A \sin 2\pi ft$, and $Q_2 \rightarrow Q_2 - A \sin 2\pi ft$.

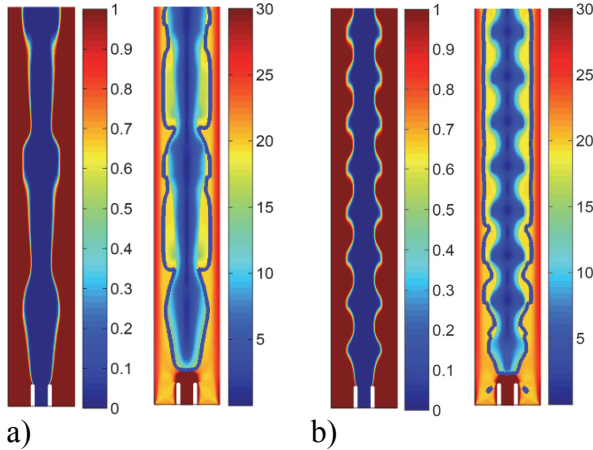


Figure 2. Example of near-net shape flows for a) $f=0.2$, b) $f=0.6$, with flow parameters $B=20$, $m=10$, $Re=20$, $A=0.1$. In each case the left colourmap shows the concentration and the right colourmap plots the magnitude of the deviatoric stress (the heavy contour line indicates the value of the yield stress).

Two example results are shown in Fig. 2, with an oscillation amplitude of 10% and two different frequencies. In both cases we observe a regular interface shape is frozen in as the flow progresses downstream. When the oscillation is established the yield surface lies outside the wavy interface indicating the presence of an unyielded sheath about the core.

Although the oscillation is sinusoidal and fairly modest the resulting interface shape is non-sinusoidal, suggesting that we are relatively far from any linear regime. Indeed the interfacial shapes achieved are quite varied.

Droplet encapsulation example flow results:

For droplet encapsulation, we have explored two methods. Firstly, we have tried increasing the oscillation amplitude, as suggested above, until the inner flow is

effectively cut. However, this method appears more complex as there can remain a thin strand of inner fluid connecting successive droplets and our numerical method is not ideal for investigating these geometries. Secondly, we have assumed an intermittent flow in the inlet before entering the main channel, i.e. for times $t > 0$, Newtonian fluid and Bingham fluid are pumped in an out phase pulsation fashion through the inner channel, while the flow rate in the outer channel is kept constant. A typical example of this is shown below in Fig. 3.

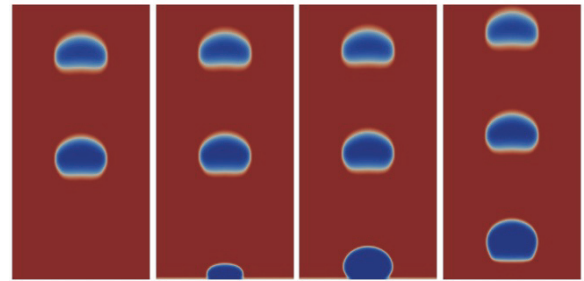


Figure 3. Typical example of droplet encapsulation showing the concentration profiles at different times for $B=20$, $m=10$, $Re=20$.

EXPERIMENTS

Experimental setup:

The basic experimental setup is illustrated schematically in Fig. 4. A Plexiglas pipe 2m long, with 25.4mm internal radius is held vertically by a collar at the lower end and attached to a drainage reservoir at the top. The outer fluid is injected into the lower end through 8 ports drilled into the collar and through the Plexiglas[®] pipe. The ports are arranged around the circumference at regular intervals. The inner fluid is injected into the pipe through a single stainless steel tube, which has its central axis aligned with that of the Plexiglas pipe. Different radii tubes may be used. Fluids are pumped to the outer injector ports using a progressive cavity pump fed by a 60 l reservoir. In the case of a

very thick fluid the reservoir can be pressurized. The inner fluid is pumped to the central injector from a 20 l reservoir using a positive displacement pump. Both pumps are directly coupled to 0.5Hp three-phase electric motors controlled by variable frequency drives.

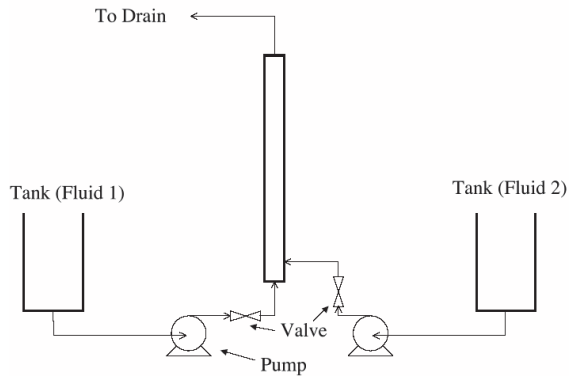


Figure 4. Flowloop schematic. Fluids 1 and 2 are inner and outer fluids respectively.

Near-net shape example flow results:

For this experimental sequence the inner fluid is a 0.3% by weight xanthan solution (Fisher Scientific Canada), with a trace amount of black food dye for visualization. The outer fluid is a 0.25% by weight Carbopol 940 EZ solution (Lubrizol Corp.) with a trace amount of Sodium Hydroxide to increase the pH to 7.0.

The flow rate of the outer fluid (Q_2) is held constant and the flow rate of the inner fluid (Q_1) is varied. The flow Q_2 is controlled by a gate valve that is actuated manually. At the start of the experiment, the two variable frequency drives are switched on and Q_2 is increased to 20 ml/s. The Plexiglas pipe is filled with fluid 2. When the pipe is full, Q_1 is increased to 15 ml/s and the multilayer flow is allowed to fully develop. After a period of about 1 minute of established flow, Q_1 is oscillated to perturb the flow.

Example results are shown in Fig. 5, where we have simply oscillated the inner fluid flow rate Q_1 between 0 and 15 ml/s as a step function (i.e. on/off), for 5s and 10s

respectively in Figs. 5a & b. We note that the interface oscillation is affected accordingly. The waveforms frozen into the interface appear to show a slight helical component.

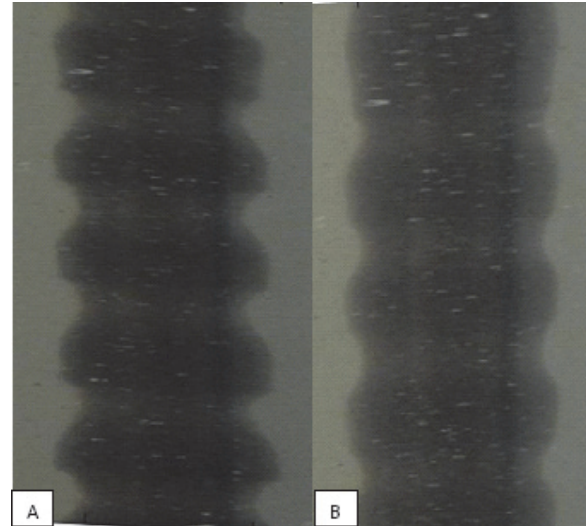


Figure 5. Example of a near-net shape frozen wavy-walled structure induced by an on/off oscillation of the inner flow $Q_1=0, 15, 0, 15, \dots$ ml/s, with $Q_2=20$ ml/s: a) oscillation time interval 5s; b) oscillation time interval 10s. The length of pipe shown is 50cm.

A different method of generating interfacial oscillations is via the rheology of the inner fluid⁵. A series of experiment has been performed with 0.75% Polyethylene Oxide solution in the inner region and 0.15% Carbopol 940 solution (yield stress fluid) at pH 5.8 in the outer region. The PEO solution is shear-thinning and exhibits significant visco-elasticity. Details of the fluid preparation and rheology are given elsewhere⁵. In this experimental sequence, the radius of the inner pipe is 1.5mm which is significantly smaller than the established radius (~ 5 mm) of the corresponding flow $(Q_1, Q_2)=(21, 30)$ ml/s. Therefore, the visco-elastic fluid experiences high stress in the inner pipe followed by flow expansion and a net relaxation of the elastic stresses. This appears to induce gentle waves with small

amplitudes at the interface. These waves are frozen at the interface by the unyielded plug region of the lubricating fluid and are convected along the pipe with the same velocity as the interface. Fig. 6 shows snapshots at 1s time intervals from a typical experiment with a frozen interfacial wave.

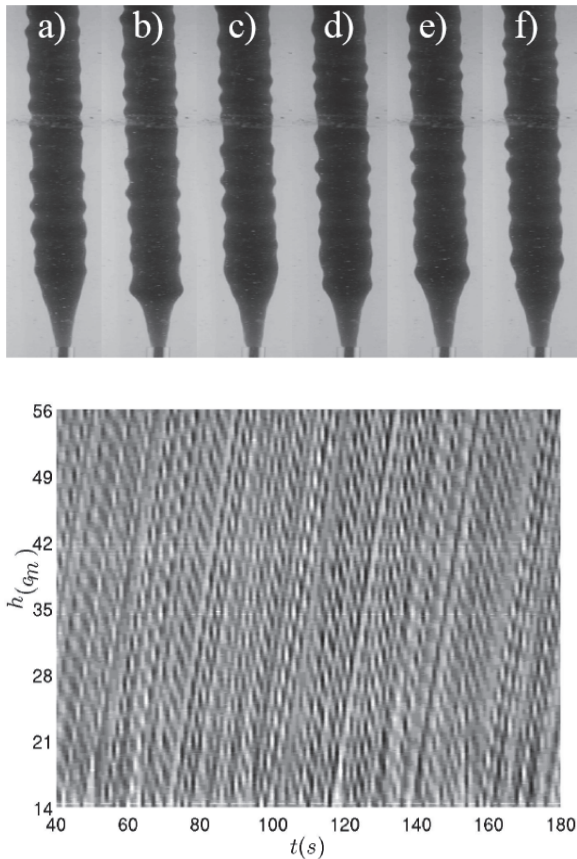


Figure 6. A typical experiment illustrating near-net shape interfacial flows induced by visco-elasticity. The interfacial wave has mean amplitude 0.7 mm and mean wave length 48 mm. Snapshots (a)-(f) show t varying from 80s to 85s with time interval of 1s. The camera captures the first 0.65 m of the pipe from the exit of the inner pipe. The bottom panel shows a spatiotemporal plot of the same experiment.

Note that the images in Fig. 6 are scaled with an aspect ratio of 15:1 to show more of the wave pattern. The bottom panel of Fig. 6 shows a spatiotemporal plot of the same experiment, focusing on a region above the

exit nozzle expansion. The image is constructed by averaging the grayscale in individual images across the pipe diameter at each height. The constant slope lines of dark and white regions confirm the constant advective velocity of the frozen interfacial waves. The waveform is fairly irregular.

Encapsulation example flow results:

A series of experiment has been performed with the same pair of fluid as for Fig. 6, but with the addition of a flow pulsation of inner and outer fluids in an out phase fashion; see Fig. 7a. The maximum flow rates are $(Q_1, Q_2) = (21, 30)$ ml/s. We initially fill the pipe with Carbopol solution before pulsating the flow rate. Figure 7b & c show the production of “pearl” and “diamond” necklaces of the inner fluid along the axis of the pipe. The only difference in is the use of inner tube inner diameters 10.74 mm and 13.86 mm respectively.

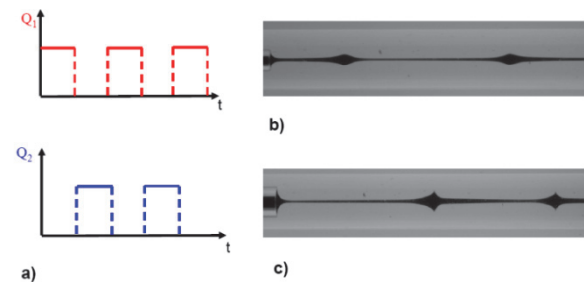


Figure 7. Examples of visco-elastic necklaces in visco-plastic fluid a) Pulsating flow rate of inner Q_1 and outer Q_2 fluid b) Pearl necklace c) Diamond necklace.

Polyethylene Oxide solution has a large extensional viscosity which prohibits mixing and keeps the interface sharp. We observe a thin “string” between the pearl and diamond droplets, probably due to the resistance of the visco-elastic fluid to the stretching motions. With inelastic core fluids, the droplets pinch-off completely. However, small disturbances can also lead to partial

mixing of the two fluids in the regimes we have studied.

SUMMARY

We have presented preliminary results of experimental and computational studies targeted at extending the visco-plastic lubrication concept¹⁻⁷ to near-net shape products and to the transport of encapsulated fluid droplets.

By introducing oscillations into an otherwise stable VPL flow we can effectively freeze into the interface a variety of wavy shapes. The oscillations may be introduced via flow rate control or by exploiting the rheological nature of the flow, e.g. Fig. 6. We can regard these as potential near-net shape methods for the production of oscillatory profiles.

More extreme controls of the inner flow rate can result in partial or full encapsulation of droplets (or “necklaces”; see Fig. 7). There remains considerable research to be done to understand quantitative differences in the shape of the interfacial waveform and the process of pinch-off in forming droplets/necklaces. This work is ongoing.

A distinction between the methods that we have illustrated and other droplet forming techniques is that length-scales are governed by the geometry of the forming device and the fluid rheological properties, rather than by capillary phenomena. This opens up possibilities for application in industries that do not operate on the micro-scale, as in most large scale industrial processing.

ACKNOWLEDGMENTS

This research has been carried out at the University of British Columbia, supported financially by NSERC. We thank Mr Ryan Yee for his help in constructing the flow loop.

REFERENCES

1. I.A. Frigaard (2001), *J. Non-Newt. Fluid Mech.*, **100**, 49–76.
2. M. Moyers-Gonzalez, I.A. Frigaard and C. Nouar (2004), *J. Fluid Mech.*, **506**, 117–146.
3. Hormozi, S & Frigaard, I.A. (2012), *J. Non-Newtonian Fluid*, **169–170**, 61-73.
4. C.K. Huen, I.A. Frigaard and D.M. Martinez (2007), *J. Non-Newt. Fluid Mech.*, **142**, 150–161.
5. Hormozi, S., Martinez, D.M. & Frigaard, I.A. (2011), *J. Non-Newtonian Fluid*, **166**, 1356-1368.
6. Hormozi, S., Wielage-Burchard, K. & Frigaard, I.A. (2011), *J. Fluid Mech.*, **673**, 432-467.
7. Hormozi, S., Wielage-Burchard, K. & Frigaard, I.A. (2011), *J. Non-Newtonian Fluid Mech.*, **166**, 262-278.
8. PELICANS is an object oriented computational platform developed at IRSN, France, to provide a general framework of software components for the implementation of partial differential equation solvers. PELICANS is distributed under the CeCILL license agreement and can be downloaded: <https://gforge.irsn.fr/gf/project/pelicans/>.